

## Short communication

Thermodynamic simulations and isothermal solubility diagrams  
as tools for slag foaming controlAna P. Luz<sup>a,\*</sup>, Thiago A. Ávila<sup>b</sup>, Paschoal Bonadia<sup>b</sup>, Victor C. Pandolfelli<sup>a</sup><sup>a</sup> Federal University of São Carlos, Materials Engineering Department, Rodovia Washington Luiz, km 235, São Carlos, SP 13656-905, Brazil<sup>b</sup> Magnesita Refratários S.A., Research and Development Center, Contagem, MG 32210-900, Brazil

Received 21 March 2011; received in revised form 9 April 2011; accepted 10 April 2011

Available online 15 April 2011

## Abstract

In this communication, the advantages and difficulties of the slag foaming process control are presented, highlighting the thermodynamic simulations role in the design of isothermal solubility diagrams (which express the relationship between MgO and FeO contents, in weight percentage, for a specific basicity and temperature). These diagrams can predict the liquid composition changes required in order to induce a longer foam lifetime at the upper surface of molten slags. Mathematical models and experimental tests have been used to understand the slag foaming phenomenon, however they do not simultaneously consider all variables involved in this process. Thus, a comparison between some experimental results and isothermal solubility diagrams was made in this work. According to this evaluation, the use of thermodynamic simulations can be a good alternative to help keeping the slag foam generation while some equipment is being used in the steel production. The use of isothermal solubility diagrams provides a clear image of which adjustments can be made in order to attain stable foam, reducing the needs for some additional experimental analyses.

© 2011 Elsevier Ltd and Techna Group S.r.l. All rights reserved.

Keywords: Slag foaming; Thermodynamic calculations; Isothermal solubility diagrams

## 1. Introduction

The slag foaming process is currently applied to some equipment for steel production [i.e., electric arc furnace (EAF), basic oxygen furnace (BOF), etc.] aiming to save energy, increase productivity, enhance the refractory service life and inhibit steel re-oxidation. However, besides its advantages, the end-users have difficulties in applying this procedure due to the lack of control of the slag chemical composition and viscosity at high temperatures [1,2].

Some work in the literature has experimentally evaluated the slag foaming phenomenon, but most of these articles only focused on the foam height analyses when an inert gas or oxygen was injected into the liquid [3–7]. The resulting foams based on this procedure are thermodynamically unstable due to their large interfacial area, leading to bubble coalescence after a short period of time.

The bubble stability is usually related to three factors:

1. Drainage of the liquid from the lamellas among the bubbles, which approaches their surfaces, resulting in their coalescence and foam collapse.
2. Coalescence due to different pressures among bubbles with different sizes, based on gas diffusion from the smaller to the larger bubbles, thus broadening their size distribution.
3. Ostwald ripening, which consists of the dissolution of small crystals or solid particles contained in the liquid and the re-precipitation of new phases at the larger crystal or solid particle surfaces [8].

Small partially hydrophobic particles and/or polymeric additives are frequently used with the aim of inhibiting the foam collapse at room temperature [8,9]. Nevertheless, new challenges and difficulties are faced at high temperatures in order to maintain foam stability.

A simplified way to indicate the foamability of liquids at high temperature consists of measuring the foaming index ( $\Sigma$ ) or the average travelling time of the gas in the generated foam.

$$\Sigma = \frac{\Delta L}{\Delta V_g} \quad (1)$$

\* Corresponding author. Tel.: +55 16 33518253; fax: +55 16 33615404.

E-mail address: [anapaula.light@gmail.com](mailto:anapaula.light@gmail.com) (A.P. Luz).

Table 1

Experimental results of the foaming index ( $\Sigma$ ) obtained at 1440 °C (1773 K) for BOF slag compositions [13].

Slag compositions	B <sub>2</sub>	wt% CaO	wt% SiO <sub>2</sub>	wt% FeO	wt% MgO	$\Sigma$
03	1.0	34.78	33.76	22.52	8.94	0.59
04	1.1	37.39	35.57	20.87	6.17	0.53
05	1.1	30.96	29.39	24.16	15.69	0.54
06	1.1	29.11	27.73	31.52	11.64	0.68
07	0.93	30.00	32.13	18.09	17.78	0.57
08	0.86	28.67	33.42	17.57	20.34	0.87
09	0.61	23.02	37.73	15.23	24.02	0.98
11	1.0	34.08	32.77	15.11	18.04	0.50
13	1.0	38.18	38.94	10.24	12.38	0.37

where  $\Delta L$  (cm) represents the foam layer thickness and  $V_g$  (cm/s) is the superficial velocity of the gas added to the system.

With the aim of improving and adding the effect of various physical slag properties in  $\Sigma$  calculation, some work highlights the search for mathematical models which express the foaming behavior in terms of slag characteristics [ $\rho$  = density (kg m<sup>-3</sup>),  $\mu$  = viscosity (Pa s),  $\gamma$  = surface tension (N m<sup>-1</sup>) and  $D_b$  = average bubble diameter (m)] [5,6]. The model proposed by Zhang and Fruehan [3] is the most accepted and used to describe the slag foamability, based on the following equation.

$$\Sigma = 115 \frac{\mu^{1.2}}{\gamma^{0.2} \rho D_b^{0.9}} \quad (2)$$

However, some difficulties remain to obtain accurate slag physical properties at high temperatures. Mathematical equations are also used to predict slag properties, but the calculated results present deviations of about  $\pm 2\%$  for density,  $\pm 10\%$  for surface tension and  $\pm 25\%$  for viscosity when compared with the actual values [10]. Therefore, some researchers prefer to experimentally evaluate the slag foamability by calculating the foaming index (Eq. (1)), when a gas phase is injected into the system, instead of using the mathematical models available (Eq. (2), for instance).

An alternative to evaluate the slag foaming phenomenon consists of analyzing phase diagrams, which can define the influence of each slag component and the combination that might result in the liquid saturation with some oxides at high temperatures. When saturated, the precipitation of solid particles of a second phase into the liquid can take place and increase the foam stability. The presence of suspended particles in the slag has a much greater impact on foaming than changing the surface tension and the slag viscosity [1]. The solid particles (commonly Ca<sub>2</sub>SiO<sub>4</sub> or MgO·FeO) act firstly, by reducing the interfacial energy of the system and changing the effective slag viscosity and, secondly, as gas nucleation sites which lead to a higher content of small gas bubbles in the liquid.

Using thermodynamic software, such as FactSage and ThermoCalc, it is possible to analyze and predict the position of the dual saturation point and the MgO and CaO saturated lines as a function of the slag basicity, temperature, oxygen partial pressure and other parameters [11,12]. When compared to some mathematical models [10], these analyses are very accurate and present an error lower than 1% when the FeO content in the slag

is less than 60 wt%. Moreover, based on these phase diagrams one can define which adjustments may be carried out in the slag composition in order to improve and optimize suitable conditions for foaming, reducing the need of experimental tests.

In this work some isothermal solubility diagrams (ISD) in the CaO–SiO<sub>2</sub>–MgO–FeO system were designed using the FactSage<sup>TM</sup> software. The thermodynamic simulations were also compared with experimental results in order to check the calculation effectiveness and the additional benefits due to the use of this tool.

## 2. Thermodynamic simulations

Some phase diagrams known as isothermal solubility (which express the relationship between MgO and FeO contents, in weight percentage, for a specific basicity and temperature) were calculated using the FactSage<sup>TM</sup> software (version 6.1, Thermfact/CRCT, Montreal, and GTT-Technologies, Aachen), which consists of a series of modules that access and manipulate thermodynamic databases. Phase Diagram module and Fact53 and FToxid databases were selected for this study, considering as possible resulting phases: gas, liquid, pure solids and various solid solutions (including spinel and other phases). After that, some slag compositions experimentally evaluated by Jung et al. [13] [Table 1, slags with binary basicity (B<sub>2</sub> = CaO/

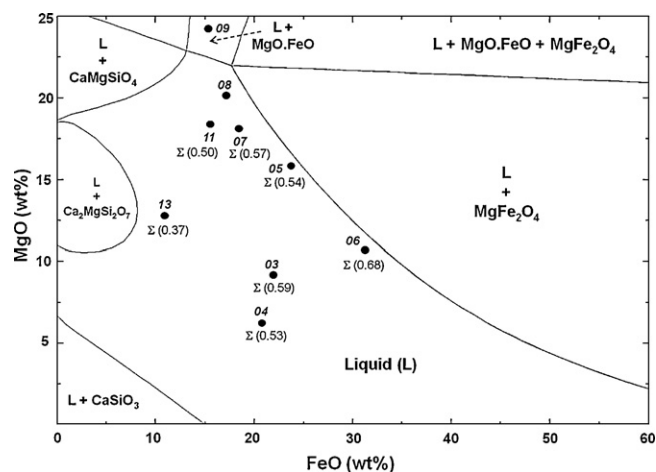


Fig. 1. ISD in the FeO–MgO–SiO<sub>2</sub>–CaO system for a basicity B<sub>2</sub> = 1, temperature = 1440 °C (1773 K) and  $p_{O_2}$  = 0.21 atm. (Foaming index attained in Table 1 are highlighted between parenthesis.)

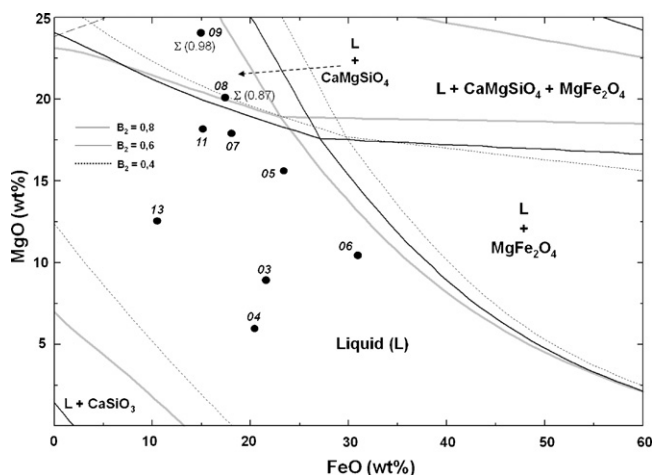


Fig. 2. ISD in the FeO–MgO–SiO<sub>2</sub>–CaO system for distinct basicities ( $B_2 = \text{CaO}/\text{SiO}_2$ ), temperature = 1440 °C (1773 K) and  $p_{\text{O}_2} = 0.21$  atm. (Foaming index attained in Table 1 are highlighted between parenthesis.)

SiO<sub>2</sub>) values in the range of 0.6 and 1.1] were plotted in the calculated diagrams (Figs. 1 and 2).

Considering the calculated isothermal solubility diagrams and the experimental  $\Sigma$  values, some analyses were carried out in order to evaluate the effectiveness of the thermodynamic simulations.

### 3. Results and discussion

Fig. 1 presents an isothermal cut for the CaO–SiO<sub>2</sub>–MgO–FeO quaternary system at the temperature of 1440 °C (1773 K) and  $B_2 = 1$ . Based on the location of the slag compositions in this ISD diagram, it was observed that those named 05, 06 and 07 are positioned close to the saturation region (spinel (MgFe<sub>2</sub>O<sub>4</sub>) + liquid) and, therefore, a greater foamability should be detected for these liquids when compared with slags 03, 04, 11 and 13. This trend was confirmed in the experimental tests according to the  $\Sigma$  values (Table 1), except for composition 03. This is because the foaming index deviation values were not presented by Jung et al. [13] and it is not possible to infer the experimental error of these measurements. As observed in Fig. 1, compositions 03, 04 and 13 are those which require greater adjustments and higher FeO contents would be necessary to provide a suitable condition for their saturation and precipitation of MgFe<sub>2</sub>O<sub>4</sub>.

On the other hand, slag compositions 08 and 09 (which present  $B_2 < 1$ , Table 1) performed best in the laboratorial analyses. Considering a condition of binary basicity equal to 1 (Fig. 1—where CaO and SiO<sub>2</sub> contents are similar in the liquid composition), slag 09 would be saturated in MgO and precipitation of MgO–FeO solid particles could take place. Nevertheless, although composition 08 would not be saturated, its location in Fig. 1 indicates that good foamability of this liquid is expected under this condition. Therefore, slight changes in the slag basicity could favour or inhibit the foaming process at high temperatures.

For example, for  $B_2$  values lower than 1 (increase of SiO<sub>2</sub> and decrease of CaO contents), compositions 08 and 09 would be saturated and located in the CaMgSiO<sub>4</sub> + L region of the ISD (Fig. 2). Moreover, based on the experimental data [13], slags 08 and 09 present viscosity values of 0.250 and 0.283 Pa s respectively. The use of the viscosity values is not enough to predict foaming behavior because, i.e., composition 07 (which had viscosity very similar to the slag 08, 0.248 Pa s) showed lower  $\Sigma$ . Most likely, the high  $\Sigma$  values collected for compositions 08 and 09 during the experimental tests are related to the presence of suspended CaMgSiO<sub>4</sub> particles, which increase the liquid viscosity, reducing the liquid drainage and the bubble coalescence for these slag compositions [1,8]. Additionally, the presence of suspended solid particles act decreasing the average free energy of the foam by reducing the gas–liquid interfacial area [8].

Changing the slag basicity values, some compositions, that firstly did not present a suitable foaming condition, can eventually be found in a region of the diagrams where the slag saturation is reached. Compositions 07 and 11, which were far from the saturation area in Fig. 1 ( $B_2 = 1$ ), are located very close to the CaMgSiO<sub>4</sub> + L region when the  $B_2$  value is reduced (Fig. 2). Therefore, ISDs could provide important information in a much simpler and accurate manner, pointing out which adjustments could be made to extend the foaming effect.

ISDs, as those presented in Figs. 1 and 2, are not frequently found in the literature, but they are important tools that can be used for controlling the slag compositions at high temperatures. Thus, some experiments carried out to evaluate the basicity, temperature and FeO and MgO contents effect on foaming behavior (as the ones performed by Jung et al. [13]) can be reduced by using thermodynamic calculations.

### 4. Conclusions

Based on the various works in the literature and due to the complexity of slag foaming phenomenon, it can be concluded that difficulties remain to define the best conditions to attain the foam generation and its stability at the upper surface of the molten slag, considering only experimental tests. Developed mathematical models are usually adjusted to a simplified situation and the prediction of slag properties can lead to inaccurate results or directions. However, the use of isothermal solubility diagrams based on thermodynamic simulations seems to be a good tool to evaluate the best conditions to induce and to keep the foam stability in steel production. The present authors have been using such tool for industrial applications with a very positive outcome.

### Acknowledgments

The authors are grateful to the Conselho Nacional de Desenvolvimento Científico e Tecnológico (CNPq) and Magnesita Refratários S.A. (Brazil) for supporting this research.

## References

- [1] E.B. Pretorius, R.C. Carlisle, Foamy slag fundamentals and their practical application to electric furnace steelmaking, in: *Proceedings of the 56th Electric Furnace Conference*, 1998, pp. 275–291.
- [2] M. Novák, J. Straka, M. Pribyl, Refractory wear in EAF viewed from the foamy–liquid slag melting processes comparison, in: *Proceedings of the 53rd International Colloquium on Refractories*, 2010, pp. 139–144.
- [3] Y. Zhang, R.J. Fruehan, Effect of the bubble size and chemical reactions on slag foaming, *Metall. Mater. Trans. B* 26 (1995) 803–812.
- [4] K. Wu, W. Qian, S. Chu, Q. Niu, H. Luo, Behavior of slag foaming caused by blowing gas in molten slags, *ISIJ Int.* 40 (10) (2000) 954–957.
- [5] K. Ito, R.J. Fruehan, Study on the foaming of CaO–SiO<sub>2</sub>–FeO slags: Part I. Foaming parameters and experimental results, *Metall. Mater. Trans. B* 20 (1989) 509–514.
- [6] K. Ito, R.J. Fruehan, Study on the foaming of CaO–SiO<sub>2</sub>–FeO slags: Part II. Dimensional analysis and foaming in iron and steelmaking processes, *Metall. Mater. Trans. B* 20 (1989) 515–521.
- [7] Y. Zhang, R.J. Fruehan, Effect of gas type and pressure on slag foaming, *Metall. Mater. Trans. B* 26 (1995) 1088–1091.
- [8] A.R. Studart, U.T. Gonzenbach, I. Akartuna, E. Tervoort, L.J. Gauckler, Materials from foams and emulsions stabilized by colloidal particles, *J. Mater. Chem.* 17 (2007) 3283–3289.
- [9] U.T. Gonzenbach, A.R. Studart, D. Steinlin, E. Tervoort, L.J. Gauckler, Processing of particle-stabilized wet foams into porous ceramics, *J. Am. Ceram. Soc.* 90 (2007) 3407–3414.
- [10] D. Lotun, L. Pilon, Physical modeling of slag foaming for various operating conditions and slag compositions, *ISIJ Int.* 45 (6) (2005) 835–840.
- [11] K.S. Kwong, J.P. Bennet, R. Krabbe, A. Petty, H. Thomas, Thermodynamic calculations predicting MgO saturated EAF for use in EAF steel production, in: *Proceedings of TMS 2009—138th Annual Meeting and Exhibition*, San Francisco, (2009), pp. 63–70.
- [12] K.S. Kwong, J.P. Bennet, Recycling practices of spent MgO–C refractories, *J. Min. Mater. Charac. Eng.* 1 (2) (2002) 69–78.
- [13] S.M. Jung, R.J. Fruehan, Foaming characteristics of BOF slags, *ISIJ Int.* 40 (4) (2000) 348–355.